Applied Thermal Engineering 253 (2024) 123843

Contents lists available at ScienceDirect

Applied Thermal Engineering

journal homepage: www.elsevier.com/locate/apthermeng

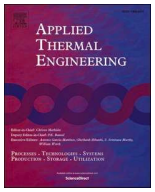

Research Paper

Parametric analysis of hybrid elastocaloric – CO_2 cooling system

Laura Nebot-Andrés [a,*], Fabio Petruzziello [b], Ciro Aprea [b], Rodrigo Llopis [a], Andrej Žerovnik [c], Angelo Maiorino [b], Jaka Tušek [c]

[a] Thermal Engineering Group, Mechanical Engineering and Construction Department, Jaume I University, Spain
[b] Department of Industrial Engineering, Università di Salerno, Via Giovanni Paolo II, 132, 84084 Fisciano, Salerno, Italy
[c] Faculty of Mechanical Engineering, University of Ljubljana, Aškerčeva 6, 1000 Ljubljana, Slovenia

ARTICLE INFO

Keywords:
CO_2
Elastocaloric
Subcooling
Modelling
Optimization

ABSTRACT

This study examines the potential application of elastocaloric refrigeration (eC) technology for the subcooling of CO_2 in transcritical single-stage refrigeration cycles. Elastocaloric refrigeration, a solid-state refrigeration technology, possesses significant untapped potential due to its environmentally friendly characteristics, primarily its lack of harmful operational fluids. However, its direct stand-alone application has been limited due to the relatively small temperature spans produced by current proof-of-concept elastocaloric devices. Efforts of the scientific community have focused on extending the temperature difference that eC systems can provide, while this work offers an alternative to that challenge, offering an application solution for the current state of technology. The study proposes for the first-time a unique integration of eC technology and CO_2 cooling systems, aiming to capitalise on the respective weaknesses of these technologies and transform them into strengths. In the proposed solution, an eC device operates as an external agent to subcool CO_2, with the objective of enhancing the energy performance of the refrigeration system. This concept is motivated by the recent advancements in CO_2 cooling systems and the growing recognition of subcooling as a promising method to boost the performance of such systems. The hybrid system's performance was evaluated across various ambient temperatures, ranging from 20 °C to 35 °C, and at an evaporating level of −15 °C. It is evaluated by means of a calculation model based on the data obtained experimentally from an elastocaloric regenerator and an experimental CO_2 plant. The system's energy efficiency was analysed in comparison to a non-subcooled CO_2 cycle, and a third cycle comprising both eC subcooling and an expander for energy recovery from the expansion process. The results demonstrated a considerable increase in the coefficient of performance (COP) with the use of eC subcooling: increments of 2.7 % at 20 °C, 4.5 % at 25 °C, 9.6 % at 30 °C and 13.1 % at 35 °C, where more significant increments were observed at higher ambient temperatures. The eC Subcooler with expander reaches increments of 7.5 %, 11.1 %, 18.1 % and 22.2 % respectively. Additionally, the eC subcooler allowed a reduction in the optimum gas-cooler pressure by up to 5 bar at the highest environment temperature. Despite these promising results, the study underscores the necessity for further optimisation and improvement of elastocaloric devices. Additionally, it emphasizes the importance of energy recovery strategies from the expansion process in transcritical CO_2 cooling system.

1. Introduction

Refrigeration is a crucial part of modern society, accounting for around 20 % of global energy consumption and contributing to 7.8 % of greenhouse gas emissions in 2018 [1]. Efforts are being made to reduce the negative impact of the vapor-compression system (VCS), the oldest electrically powered technologies still in use, with no viable alternative [2], by decreasing the use of high-global-warming-potential (GWP) refrigerants like hydrofluorocarbons (HFCs) [3,4]. F-Gas Regulation was one of the keys of European union to prevent the release of 80 billion tonnes of CO_2 equivalent by 2050 and limit global temperature rise below 2 K. Alternative refrigerants such as hydrocarbons (HCs) and CO_2 are being introduced, but they have their limitations, such as flammability and high operating pressures. Innovations like ejectors [5] and new cycle configurations [6,7] are being developed to address these limitations and improve the efficiency of CO_2 refrigeration systems. Among these innovations, subcooling of CO_2 has shown great potential

* Corresponding author.
E-mail address: lnebot@uji.es (L. Nebot-Andrés).

https://doi.org/10.1016/j.applthermaleng.2024.123843
Received 8 April 2024; Received in revised form 4 June 2024; Accepted 28 June 2024
Available online 30 June 2024

Nomenclature

CO_2	carbon dioxide
BP	back-pressure valve
COP	coefficient of performance
CSSR	Caloric solid-state refrigeration
$\bar{c}_{eCM}$	average specific heat of elastocaloric material
DMS	dedicated mechanical subcooling
eC	elastocaloric
EXV	electronic expansion valve
f	frequency, Hz
GWP	global warming potential
h	enthalpy, kJ/kg
HC	hydrocarbons
HFC	hydrofluorocarbon
IMS	Integrated mechanical subcooling
M	mass, kg
$\dot{m}$	mass flow, kg/s
P	pressure, bar
P_c	power consumption, kW
q	specific cooling capacity, kW/kg
$\dot{Q}_0$	cooling capacity, kW
SUB	subcooling degree, K
T	temperature, °C
TRL	technological readiness level
TS	thermoelectric cooling
VCS	vapour-compression system
w	specific work, kW/kg

Subscripts

a	referring to points in Fig. 2a
act	actuator
app	approach
b	referring to points in Fig. 2b
c	referring to points in Fig. 2c
cold	refers to the cold side
eC	referring to elastocaloric device
env	referring to the environment
exp	expander/experimental
gc	gas-cooler
hot	refers to the hot side
i	inlet
o	outlet
0	referring to the evaporator
me	mechanical
net	net electrical
SH	superheating
sub	subcooling
suc	suction

Greek symbols

ΔT_{ad}^{-}	adiabatic temperature change upon unloading
$\Delta T_{app,eC}$	approach temperature in subcooler
ΔT_{span}	temperature span, K
η_C	overall effectiveness of compressor
v	specific volume, m^3/kg

[8]. Subcooling is performed at the exit of the gas-cooler by means of an auxiliary cycle that performs heat rejection to the same heat sink as the main cycle. This entails and increment in the specific cooling capacity, a reduction of the optimum pressure and thus a reduction of the specific compression work. If the COP of the auxiliary cycle is higher than the COP of the main cycle, also an increment in the overall COP is obtained [9]. CO_2 Subcooling has been proved experimentally with vapour compression systems, where the efficiency increase in relation to the parallel compression system reached up to 17.5 % [10], and also this technique has future potential to be the nexus between the emerging caloric refrigeration systems with vapour compression ones, as more than 9 % increase in COP has been predicted simply hybridizing the existing prototypes [11].

Fig. 1 shows the experimental COP obtained by different technologies as a function of the temperature span between the heat sink and heat source. The dedicated mechanical subcooling system (DMS) [12] and integrated mechanical subcooling system (IMS) [13] can reach COPs up to 6, providing temperature spans between 25 K and 45 K. However, some of these points are marked with a cross because the compressor is out of operating range, therefore, for these specific cases it is necessary to develop compressors that can work in this range (high suction temperatures and compression ratios below 1.5) [14], which has not been considered up to now. New cooling production methods, such as elastocaloric and magnetocaloric, which belong to the group of caloric solid-state refrigeration (CSSR) technologies [15] have shown high COP with lab assemblies but they have not provided sufficient temperature span to be yet widely useful as stand-alone systems and have low TRL values (TRL 2–3). Thus solid-state refrigeration technologies have high potential to be considered as a subcooling systems, as they are environmentally benign and can reach high COP values at small temperature spans. For example, as shown in Fig. 1 thermoelectric cooling (TS) can reach COP up to 6 at 15 K of a temperature span [15]. CSSR, cutting-edge technologies, are still in process of development [16]. Caloric technologies are based on solid-state phase transitions in

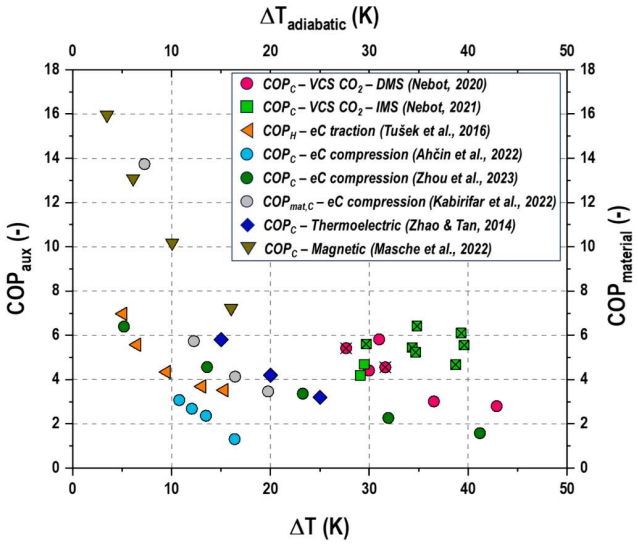

Fig. 1. Refrigerating and heat pumping COP of subcooling systems used in CO_2 transcritical plants and performance.

ferroic materials, which are triggered by external field (magnetic, electric, or mechanical) [17,18]. We can thus distinguish between magnetic (magnetocaloric) refrigeration, electrocaloric refrigeration [19], elastocaloric refrigeration [20] and barocaloric refrigeration [21]. The most developed among caloric technologies is magnetic refrigeration, with up 100 prototypes developed in universities and laboratories around the world, followed by elastocaloric refrigeration [22].

As seen from Fig. 1 the most efficient magnetic refrigeration device developed so far can reach COP of up to 16 at 4 K of the temperature

span and up to 7 at 16 K of the temperature span [23]. Mostly due to hysteresis losses in most elastocaloric materials, the prototypes of elastocaloric devices currently still less efficient compared to magnetic refrigeration, but their main advantage compared to magnetic refrigeration is that they are not based on expensive rare-earth materials. Also, in latest researches more fatigue-resistant materials are identified [24,25]. Fig. 1 shows the COP values of three different elastocaloric prototypes based on tensile and compressive loading [26–28]. The most efficient elastocaloric devices [26,28] can reach COP of up to 7 at 5 K of the temperature span and of around 4 at around 15 K of the temperature span. As a comparison, Fig. 1 also shows the material COP values as a function the adiabatic temperature change in the material (on the secondary axis and in gray color) of the most widely studied elastocaloric material (i.e., Ni-Ti alloy). The material COP presents the ratio between cooling energy generated due to the elastocaloric effect and the hysteresis loop area, which presents the required input work (assuming a complete work recovery of the energy released during the unloading) [29]. The material COP values thus presents the maximum COP that can be potentially reached in an elastocaloric device if other losses such as heat transfer and/or viscous would be minimized. High material COP values (around 14 at 7 K of the temperature span) therefore means that there is still significant room for improvements in designing more efficient elastocaloric devices in the future, especially considering recent development of elastocaloric materials with smaller hysteresis losses, e.g. [30,31], which can further improve the material COP values.

The first idea of combining vapor compression and elastocaloric cooling technologies was presented by Žerovnik & Tusek in 2016 [32]. As described, elastocaloric technology can provide high COP when the temperature span is small. And this temperature span (between 5 to 10 K for caloric systems [11]) matches with the temperature difference between the heat rejection temperature and the gas-cooler outlet temperature in CO_2 refrigeration systems, which makes hybridization of technologies possible and requires further investigation.

This paper presents the possibility of combining elastocaloric systems with CO_2 refrigeration cycles. The objective of this work is to show and evaluate the possibilities of merging CO_2 VCS technology with elastocaloric refrigeration systems. We present the possibility of hybrid cooling cycles, where a basic CO_2 cycle is combined to an elastocaloric refrigeration device to perform subcooling. Combining both technologies into a hybrid cooling system allows to transform the disadvantages of each technology into advantages, which leads to a more efficient and environmentally friendlier cooling system. The main objective of this work is to evaluate the potential of this hybrid technology also considering the use of an expander [33] to activate (load and unload) the elastocaloric device, for different environment temperatures and quantify the improvement with respect to a basic CO_2 refrigeration cycle.

2. Methodology

To explore the benefits of the hybrid eC-CO_2 cooling cycle, three cycles are contrasted from a theoretical approach:

- Baseline cycle: single-stage cycle with double-stage expansion (Fig. 2a): Simple vapour compression refrigeration cycle in which CO_2 is expanded in two stages: the first expansion valve (BP) allows the high pressure to be controlled and thus optimised, while the second expansion valve (EXV) controls the useful superheat.
- Cycle with eC subcooler: baseline cycle incorporating and eC subcooler driven by external mechanical energy (Fig. 2b): The main components of the cycle are the same as above, but an additional heat exchanger is added. This serves as thermal connection between the vapour compression cycle and the elastocaloric system. In this heat exchanger, located at the outlet of the gas-cooler, the CO_2 subcooling takes place, produced by the eC device.
- Cycle with expander and eC subcooler (Fig. 2c): This third configuration is intended to recover the energy from the second expansion stage and replaces the EXV valve with an expander. The expander is connected to the eC device and the recovered mechanical energy is used to partially drive the eC subcooler.

As eC subcooler, the experimental prototype developed by Tusek et al. [26] is considered, which is detailed below.

2.1. Mathematical modelling

COP, defined as the ratio between the cooling capacity provided by the refrigeration cycle in the evaporator and the input power to run the system (Eq. (1)), is considered as objective function. Cooling capacity and electrical power consumption are defined in Annex I as well as the calculations needed to obtain these values for each of the cycles. In this section, the obtained equation to calculate the COP of each cycle as a function of enthalpies values is presented.

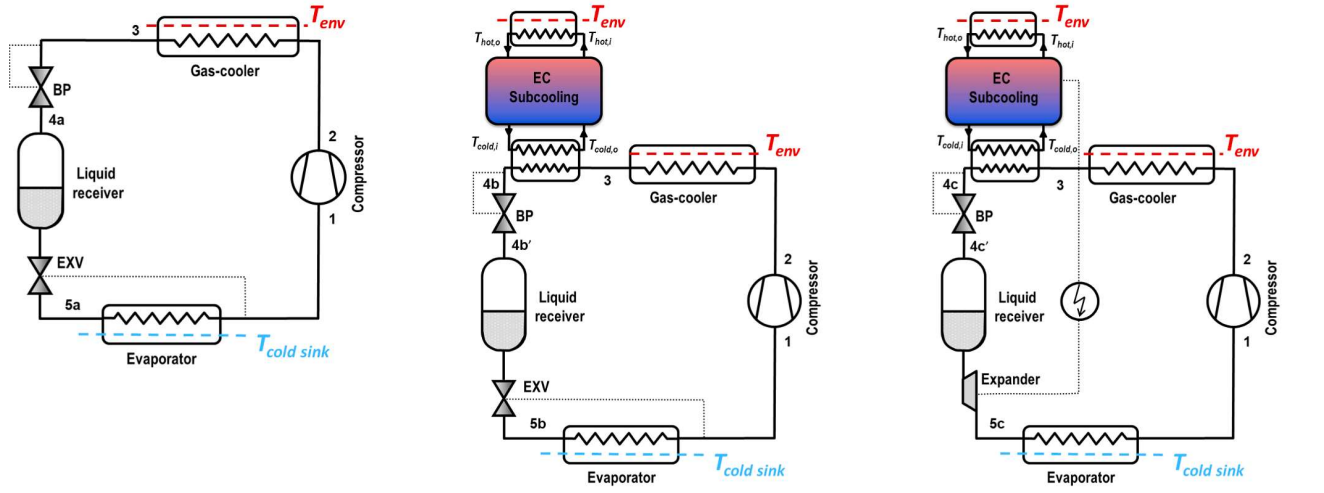

a - cycle with double-stage expansion

b - cycle with eC subcooler

c - cycle with expander at 2nd expansion stage and eC subcooler

Fig. 2. Thermodynamic cycles considered in this work.

$$COP = \frac{\dot{Q}_O}{P_c} \quad (1)$$

Each of the evaluated cycles shown in Fig. 2 and have the following common thermodynamic states: the enthalpy at compressor suction (point 1 in Fig. 2); the discharge enthalpy (point 2 in Fig. 2) and temperature at the exit of the gas-cooler.

– **The baseline cycle (**Fig. 2**a)**, the COP for the baseline cycle can be written by Eq. (2).

$$COP_a = \frac{h_1 - h_{5a}}{h_2 - h_1} \quad (2)$$

– **Cycle with elastocaloric subcooler (**Fig. 2**b).** The eC subcooler cools down the CO_2 at the exit of the gas-cooler. Therefore, the COP of the cycle with eC subcooler can be expressed by Eq. (3), where the COP of the eC device (COP_{eC}) are calculated through the values obtained experimentally (Table 1) and where q_{sub} is the specific heat extracted with the subcooling system. More details about the calculation are presented in Annex I.

$$COP_b = \frac{\dot{Q}_{O,b}}{P_C + P_{eC,b}} = \frac{h_1 - h_3 + q_{sub}}{h_2 - h_1 + \frac{q_{sub}}{COP_{eC}}} \quad (3)$$

– **Cycle with expander at the 2nd expansion stage and elastocaloric subcooler (**Fig. 2**c).** Finally, this configuration uses both sub-systems: energy recovery in the 2nd expansion stage through a generic expander and electric generator that is used to drive the eC subcooler, which further cools down the refrigerant at the exit of the gas-cooler for a certain subcooling degree. This cycle assumes that the energy recovered by the expander after conversion to electric power is used to partially drive the eC device that requires larger input power to provide the desired subcooling power. The calculation of the electric power values is presented in Annex I and the COP of this cycle can be expressed with Eq. (4).

$$COP_c = \frac{\dot{Q}_{O,c}}{P_{net,c}} = \frac{h_1 - h_3 + q_{sub} + +\eta_{exp}\cdot(h_{4c'} - h_{5c,s})}{h_2 - h_1 + \frac{q_{sub}}{COP_{eC}} - (h_{4c'} - h_{5c})\cdot\eta_{me}} \quad (4)$$

2.2. Model of the elastocaloric device

The measured experimental performance of an eC heat pump prototype was used as reference to simulate the eC subcooler. Tušek et al. [26] reported experimental performance data of a small-scale prototype, where the specific parameters were related to the amount of elastocaloric material used in the prototype. The prototype was based on the active elastocaloric regenerator made of thin Ni-Ti sheets with the thickness of 0.25 mm and the spacing between them (fluid-flow channels) equal to 0.25 mm, which resulted in 50 % regenerator porosity. The prototype was working in a heat-pumping mode and it tested at two operating frequencies and different strain values, whose experimental data are reported in Table 1. From this data the device performance operating in refrigerating mode was calculated using basic thermodynamic relations (by neglecting the impact of hysteresis losses of eC material). Eqs. (5)–(10) were used to calculate the refrigeration COP, the mechanical specific input work, and the specific cooling capacity of the device, respectively.

$$COP_{c,exp} = COP_{h,exp} - 1 \quad (5)$$

$$w_{exp} = \frac{q_{h,exp}}{COP_{h,exp}} \quad (6)$$

$$q_{c,exp} = q_{h,exp} - w_{exp} \quad (7)$$

To make the analysis and optimization procedure more comprehensive, the performance of the eC device was linearized over a wider temperature span. ΔT_{span} and COP_C interpolated for a given applied strain of 3 % and displaced fluid volume ratio equal to 1 are shown in Fig. 3 as a function of the cooling capacity per unit of eC material. Only the operation at a frequency of 1/8 Hz was used in this work. Displaced fluid volume ratio is defined as ratio of the volume of the heat transfer fluid pumped through the regenerator in a single heat transfer period with the volume of the fluid in the regenerator. According to the experimental findings of magnetic refrigeration technology (analogue solid-stage refrigeration technology to elastocalorics), the dependency of the temperature span and COP on the specific cooling power can be assumed with good approximation to be linear (for a given magnetic field change and utilization factor) [34]. To generate the linear $\Delta T_{span} = f(q_{C,\mathrm{exp}})$ relation two characteristic points are required: one point was interpolated from the experimentally measured temperature span and the corresponding specific cooling power (the specific cooling power was calculated by Eqs. (5)–(7) of the eC prototype [26], while the other corresponds to the maximum specific cooling power at zero temperature span and was calculated using Eq. (8). Here, it is assumed that at the zero temperature span the entire eC effect upon unloading contributes to the cooling power. In Eq. (8), $\bar{c}_{eCM}$ is the average specific heat of the elastocaloric material (480 $J{\cdot}kg^{-1}{\cdot}K^{-1}$) and ΔT_{ad}^{-} is the adiabatic temperature change during the unloading for a fixed strain value, which was for the applied elastocaloric material equal to 10.3 K at 3 % of strain [26].

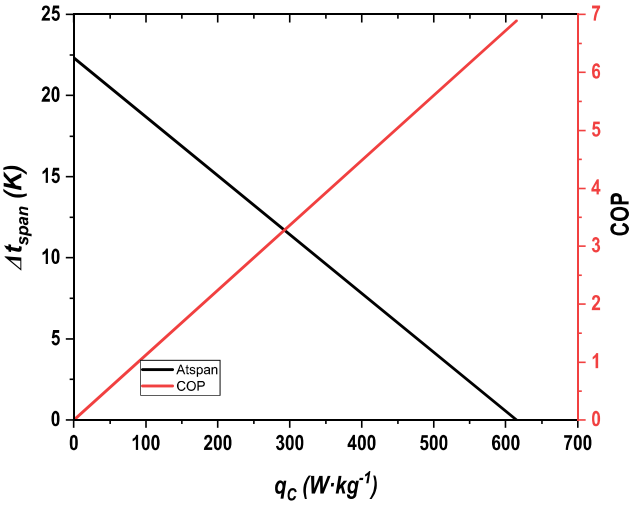

Fig. 3. Linear dependence of Δt_{span} and COP_h on the specific cooling power for 0.125 Hz of operating frequencies at U = 0.3.

Table 1
The experimental characteristics of the eC device (measured and/or calculated by Eqs. (27) and (28)) used as the input data to the model [26].

Freq. (Hz)	Strain (%)	ΔT_{span} (K)	$q_{h,exp}$ ($W{\cdot}kg^{-1}$)	w_{exp} ($W{\cdot}kg^{-1}$)	$q_{o,exp}$ ($W{\cdot}kg^{-1}$)	$COP_{h,exp}$ (−)	$COP_{c,exp}$ (−)
1/8	1.68	5.5	171.2	31.3	139.9	5.5	4.5
	2.28	8.8	273.6	56.4	217.2	4.8	3.8
	2.85	11.6	365.3	83.9	281.4	4.3	3.3
	3.43	13.3	403.6	106.6	296.9	3.8	2.8

$$q_{C,max} = f \cdot \bar{c}_{eCM} \cdot \Delta T_{ad}^{-} \quad (8)$$

Similarly, the linear $COP_{C,\exp} = f(q_{C,\exp})$ relations were constructed based on two characteristics points, where one is at zero specific cooling power, which corresponds to zero COP_C values, while the other was interpolated from the experimentally measured specific cooling power – COP_C characteristics (the specific cooling power was calculated by Eqs. (27)–(29)) of the eC prototype [26]. Fig. 3 shows the linear $\Delta T_{span} = f(q_{C,\exp})$ *and* $COP_{C,\exp} = f(q_{C,\exp})$ relations for the operating frequency used at the input data to the model.

2.3. Thermal-mechanical coupling

Although a single active eC regenerator was used to measure the experimental performance of the elastocaloric material, a real implementation, as suggested by Kabirifar et al. [29] will be built with several phase-shifted eC regenerators, where one set of regenerators is loaded and the other simultaneously unloaded. In such design the overall input work is smaller, since energy released during the unloading of one regenerator can be used directly for loading of another regenerator and vice versa. By using a rotary driving system and several continuously operated phase-shifted regenerators, theoretically (excluding the friction losses) the entire energy released during the unloading can be recovered and used as an input work for another regenerator that is being loaded in that time or in the next eC cycle. Therefore, for the purpose of this work, it is assumed that the entire energy released during the unloading can be fully recovered and the input work is equal to the difference between loading and unloading energy (i.e., hysteresis). It should be noted that this assumption has already been included in the COP values of the elastocaloric device under consideration presented in Table 1.

However, neglecting the thermal losses, a required subcooling specific cooling power (q_{sub}) equals to the specific cooling capacity provided by the eC subcooler (Eq. (9)); the net input work to the eC device can be evaluated with Eq. (10) – assuming perfect work recovery, where $\eta_{e,act}$ accounts for the efficiency of the electrical-to-mechanical actuator. In addition, the COP (electric based) of the eC subcooler can be calculated by Eq. (11).

$$q_{sub} = q_{o,exp} \quad (9)$$

$$w_{eC} = \frac{w_{exp}}{\eta_{e,act}} \quad (10)$$

$$COP_{eC} = \frac{q_{o,exp}}{w_{eC}} \quad (11)$$

Finally, to provide the required absolute cooling capacity by the eC subcooler, the required amount of elastocaloric material is calculated as:

$$M_{eC} = \frac{\dot{m} \cdot q_{sub}}{q_{o,exp}} \quad (12)$$

To allow hybridization, the operating temperatures of the refrigeration cycle and of the eC refrigerator should be matched. Fig. 2 schematizes the thermal coupling of both subsystems for subcooling purposes. Hot outlet temperature ($T_{hot,o}$) and cold inlet temperature ($T_{cold,i}$) of the subcooler were estimated using a fixed approach temperature ($\Delta T_{app,eC}$), as shown by Eqs. (13) and (14), respectively. Finally, the temperature span provided by the EC subcooler (ΔT_{span}) is defined by Eq. (15).

$$T_{hot,o} = T_{env} + \Delta T_{app,eC} \quad (13)$$

$$T_{cold,i} = T_4 - \Delta T_{app,eC} \quad (14)$$

$$\Delta T_{span} = T_{hot,i} - T_{cold,i} \quad (15)$$

The developed model is entirely generic and adaptable for any input value. It is developed with Matlab and Refprop [35], that allows to obtain the thermodynamic properties of CO_2. Based on the input data, the model has been programmed to optimize the two key variables in the cycles, the optimum subcooling degree and optimum heat rejection pressure that maximize the COP, as discussed in Section 3.

3. Results and discussion

In this section, the optimized main results of the hybrid device working at different conditions are presented. First, the evaluation assumptions are stated and how the operation of the system is optimized is described. Then, the discussion of the results focuses on the main energetic parameters and the optimum parameters needed to achieve them.

3.1. Assumptions for the analysis

The following assumptions were considered for the simulations:

- External conditions: CO_2 refrigeration cycle was simulated at a constant evaporating temperature of −15 °C and for a heat rejection temperature between 25 and 40 °C.
- Simulation conditions: cycles were evaluated only in transcritical conditions, assuming an approach temperature in gas-cooler ($\Delta T_{gc} = T_3 - T_{env}$) of 2 K; approach temperature in subcooler ($\Delta T_{app,eC} = T_{4,i} - T_{cold,i}$) in the cold and hot sides of 2 K, due to the good thermal transfer of carbon dioxide at the supercritical region [36,37]. Superheating degree in the evaporator (ΔT_{SH}) was set to 5 K.
- Component's efficiencies: compressor overall efficiency was modelled using Eq. (I. 5) from Annex I, expander's isentropic efficiency (η_{exp}) was set at 40 % [33]; mechanical-to-electric conversion efficiency (η_{me}) was of 95 %; electric-to-mechanical conversion efficiency to drive the eC device ($\eta_{e,act}$) was set at 75 %.
- eC subcooler: a perfect work recovery during the unloading was assumed (neglecting friction losses and efficiency of the driving system).

3.2. Optimization of refrigeration cycles

CO_2 transcritical refrigeration cycles with subcooling must be optimized in terms of gas-cooler pressure (p_{gc}) and subcooling degree (SUB) to reach the maximum COP for each condition; while for baseline CO_2 cycles, only the high pressure must be optimized. Thus, in the case of performing the subcooling with an eC subcooler, both pressure and subcooling need to be optimized.

Fig. 4 illustrates the optimization for the system with eC subcooler activated externally (left) and with eC subcooler partially activated with an expander (right) for an environment temperature of 35 °C, evaporation of −15 °C, V*=1, and frequency of 1/8 Hz. As it can be seen, COP dependents on the SUB and the p_{gc}, and thus the working condition that provides maximum COP (red points) can be found. Comparing the optimization with and without expander, the trend is the same, but the use of the expander continually increases the COP to a certain extend. In Fig. 5, the main differences among the cycles can be observed. The *p-h* diagrams at optimum conditions (red points in Fig. 4.) for the conditions T_{env} = 35 °C, T_o = −15 °C, V*=1, f = 1/8 Hz, are depicted. The main effect of the subcooling is the increase in the specific cooling capacity and the decrease of the optimum pressure, which is obtained for both cycles with eC. The use of the expander increases a bit more the specific cooling capacity due to the isentropic behavior of the second expansion, while the other points remain the same.

Table 2 summarizes the main results of the evaluated conditions presented in Fig. 5. The main differences due to the use of the expander are observed in the compressor specific work that is slightly lower than that of the eC subcooler without expander (due to the energy recovered)

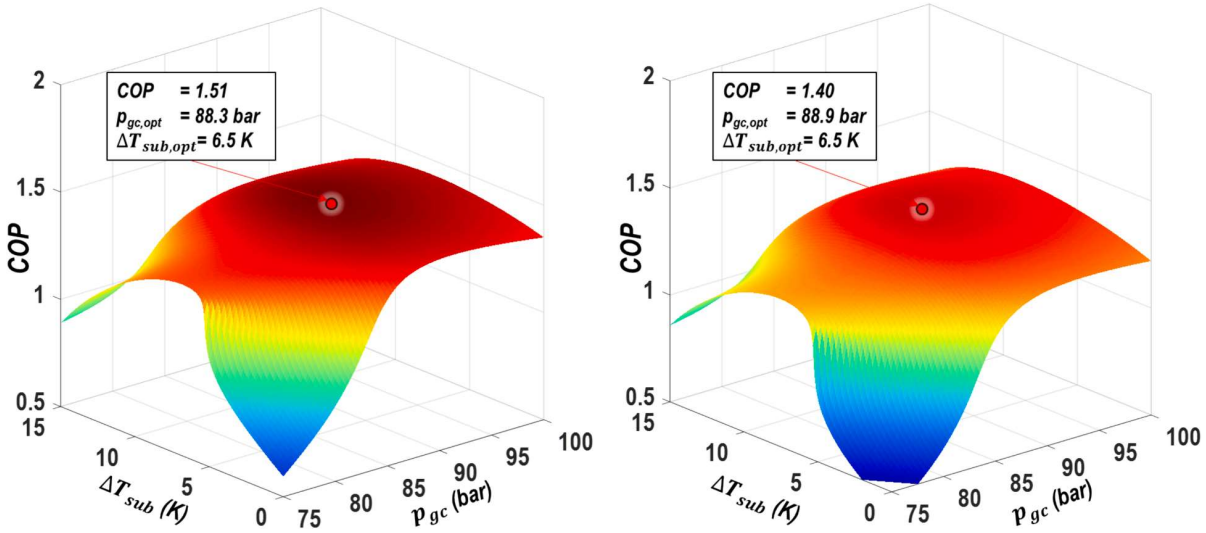

Fig. 4. COP evolution as function of subcooling degree and heat rejection pressure at T_{env} = 35 °C, T_o = −15 °C.(left: with eC subcooler activated externally; right: with eC subcooler partially activated with expander in the second expansion stage).

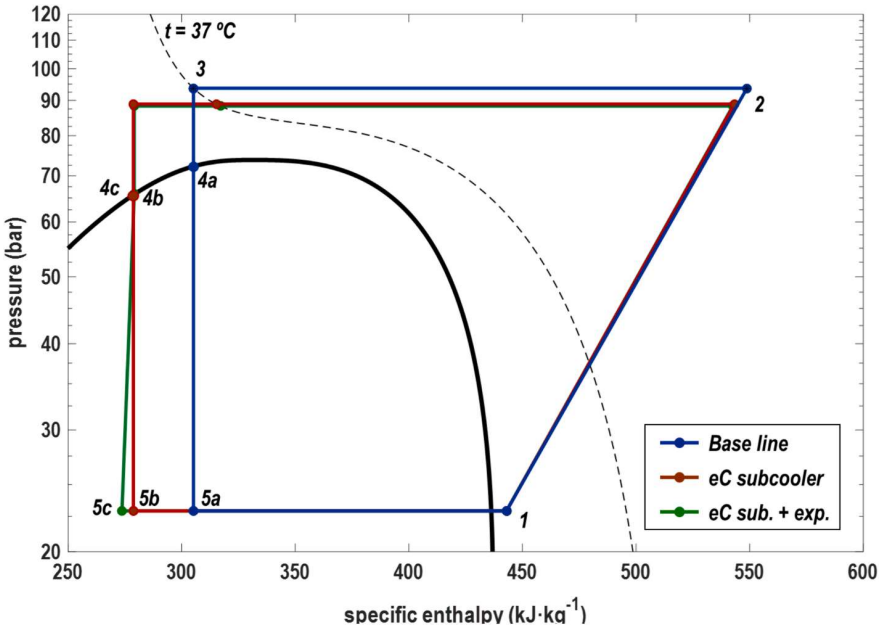

Fig. 5. Pressure enthalpy diagram at optimum conditions at T_{env} = 35 °C, T_o = −15 °C.

Table 2
Performance comparison at optimum conditions at Tenv = 35 °C, To = -15 °C.

	COP	Pgc (bar)	SUB (K)	w_C (kJ·kg^{-1})	w_{eC} (kJ·kg^{-1})	q_o (kJ·kg^{-1})	q_{sub} (kJ·kg^{-1})	w_{exp} (kJ·kg^{-1})	COP_{eC}	ΔT_{span} (K)
Base	1.236	93.72	–	111.50		137.8	–	–	–	–
eC subcooler	1.398	88.89	6.535	105.55	11.90	164.2	36.4	–	3.06	10.5
eC sub. + exp.	1.511	88.29	6.533	105.27	11.91	169.3	38.3	5.14	3.21	10.5

and in the COP of the eC device: 3.06 without expander and 3.21 with expander. Regarding the optimization parameters, optimum subcooling degree is the same in both cases as well as the temperature span, that is directly related to the SUB. In terms of optimal pressure, the device with expander has its optimum at a pressure 0.6 bar lower than the eC device, both being around 5 bar lower compared to the cycle without subcooling.

3.3. *Results at optimum conditions*

Once the cycle optimization process is known, this section presents the optimal results (those that give the maximum COP according to the procedure detailed in subsection 3.2) for ambient temperature conditions between 20 and 35 °C and −15 °C of evaporation temperature. The analysis was performed for a device providing a cooling capacity of

1 kW. The required quantity of elastocaloric material will depend on the cooling needs.

Fig. 6 shows the COP evolution and its increment in relation to the base system operation for the three studied cycles. The COP of the three systems follow the same trend, where one can see that subcooling improve the baseline COP for all environmental temperatures. In the case of the eC Subcooler, COP decreases from 2.19 to 1.40 when the temperature is increased from 20 °C to 35 °C, while in the case of eC Subcooler and expander from the COP decreases from 2.29 to 1.51, while the base cycle reaches COPs from 2.14 to 1.24, respectively.

As seen in Fig. 6, the use of the eC and the expander enhances the COP compared to the baseline, the COP increments calculated as:

$$\Delta COP(\%) = \frac{COP_{b/c} - COP_a}{COP_a} \quad (16)$$

The eC subcooler allows to obtain COP increments of 2.7 % at 20 °C, 4.5 % at 25 °C, 9.6 % at 30 °C and 13.1 % at 35 °C, while the eC Subcooler + Expander reaches increments of 7.5, 11.0, 18.1 and 22.2 % respectively. It can be concluded that the use of the eC is more convenient in the case of higher environment temperatures although it is positive in all the cases.

As mentioned before, to obtain the maximum COP, subcooling degree and pressure must been optimized. Subcooling degree has a direct effect on the temperature span and thus on the COP of the eC device (COP_{eC}). Fig. 7 presents these parameters for the case of the cycle with eC subcooler. As it can be seen, the trend of the SUB and the ΔT_{span} is exactly the same, but the ΔT_{span} is always 4 K higher, due to the temperature approaches considered in the heat exchangers. The optimum subcooling degree is higher when the ambient temperature is higher, also observed in other subcooling devices [12,38,39]. On the contrary, higher the environment temperature is, lower the COP_{eC} would be, because as stated in the previous sections, the COP_{eC} is higher at smaller temperature spans.

Optimum gas-cooler pressure is depicted in Fig. 8 for lower temperatures, 20 °C and 25 °C, the optimum pressure is 75 bar for all the cycles, corresponding to the lowest evaluated pressure, to assure transcritical conditions. Above 25 °C, the optimum pressure increases as the environment temperature does, but a clear reduction can be observed between the devices with subcooling with respect to the base cycle, up to a reduction of around 5 bar at 35 °C. Comparing both subcooled cycles, the one with the expander has always slightly lower optimum pressure.

As mentioned in Section 2.3, the absolute cooling capacity will depend on the quantity of elastocaloric material placed on the eC

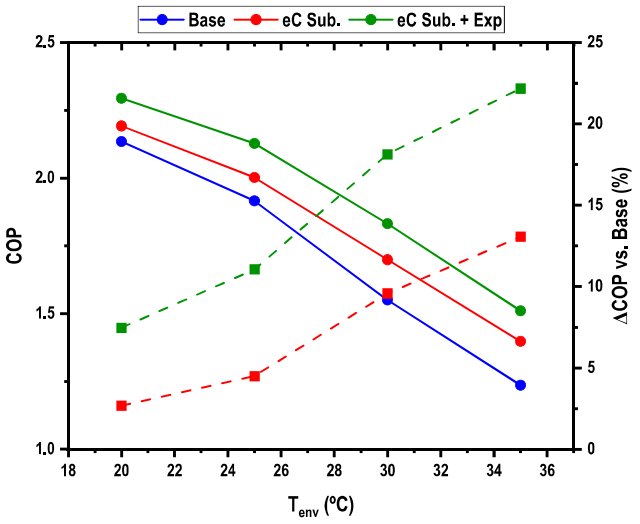

Fig. 6. COP and COP increment vs. Base at optimum conditions for different T_{env} ($T_o = -15$ °C).

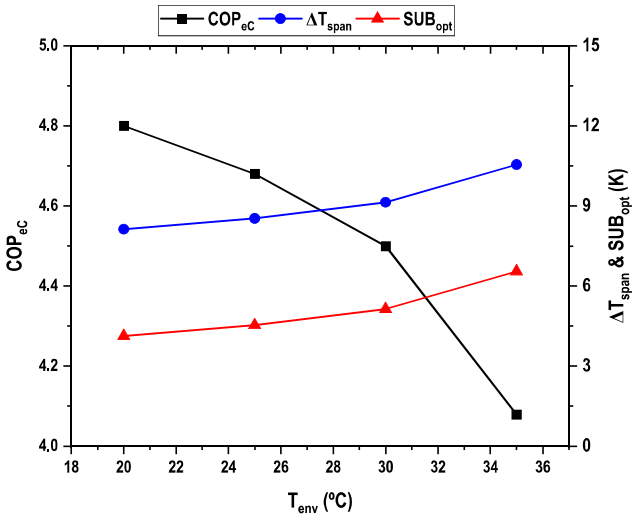

Fig. 7. Temperature span, subcooling degree and COP of the eC cycle for evaluated T_{env} environment temperatures at $T_o = -15$ °C.

subcooler. The required amount of elastocaloric material, Eq. (12), needed to produce 1 kW in each of the evaluated conditions is presented in Fig. 9. As it can be seen, higher the environment temperature is, larger the mass of eC material would be needed in the subcooler. It is because the optimum subcooling degree is higher and thus more elastocaloric material is needed to achieve this. In Fig. 7 it has been demonstrated that the eC Subcooler with expander is more interesting as it offers higher increments and also entails a higher reduction of the optimal pressure (Fig. 8); however, more material is needed in comparison to the cycle without expander. Therefore, the decision between one system and another will depend on the needs and budget of each application.

Table 3 compares different types of subcooling systems working under the same conditions. For an ambient temperature of 25 °C and an evaporation level of −15 °C, the COP, optimum pressure and subcooling degrees of the cycles with parallel compression, dedicated and integrated mechanical subcooling, magnetic refrigeration subcooling and elastocaloric refrigeration subcooling with and without expander are detailed.

As it can be seen, solid state technologies can offer higher COP compared to the existing subcooling cycles. Elastocaloric subcooling is near the COP of magnetocaloric subcooling [11] and when using the expander, it overpasses it. Regarding the optimum gas-cooler pressure, no important differences are noticed between the cycles, however, the subcooling degree needed for the elastocaloric technology is much smaller compared to others [10]. Table 4 shows the same comparison but considering an environment temperature of 35 °C. As it can be seen, the eC continues to be competitive and for these conditions overpasses the performance of the MC subcooling.

4. Conclusions

Elastocaloric refrigeration, a solid-state refrigeration technology, still underdeveloped, is a technology with a promising future because it can achieve much higher COPs than vapor compression technologies. However, it has not yet been possible to develop prototypes that can provide a sufficiently large temperature difference for current refrigeration applications.

This works presents a new application for elastocaloric refrigeration in which its unique characteristics fit perfectly to the needs of this application: subcooling CO_2 in refrigeration cycles. This is a solution that solves the problem of this technology and opens the door to a new development opportunity. This solution takes advantage of the weaknesses of each technology and turn them into positive features. An

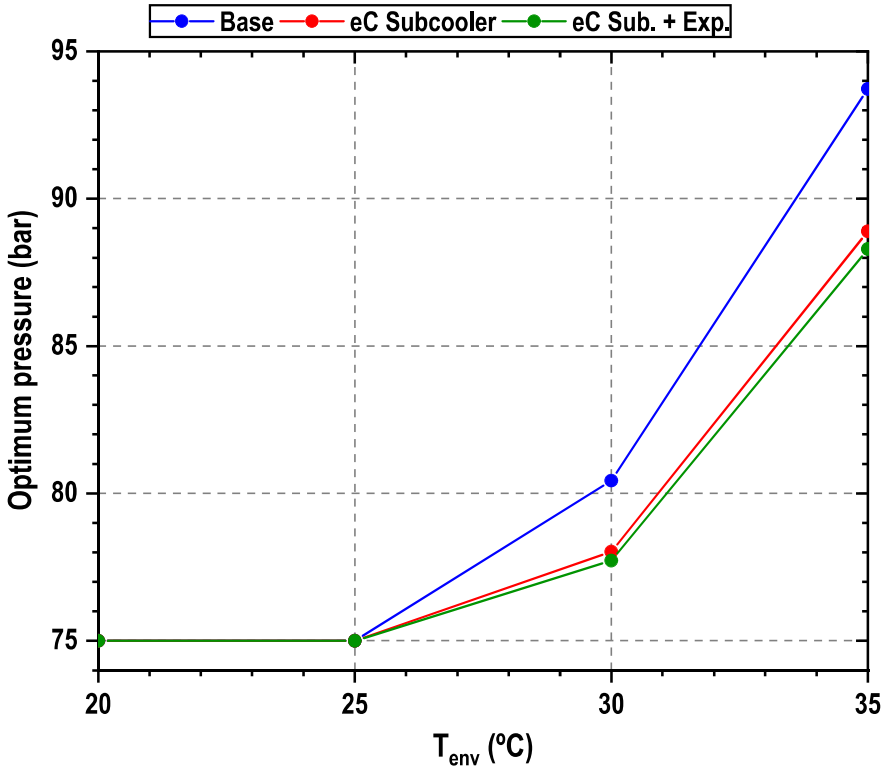

Fig. 8. Optimum pressures depending on T_{env} at $T_o = -15$ °C.

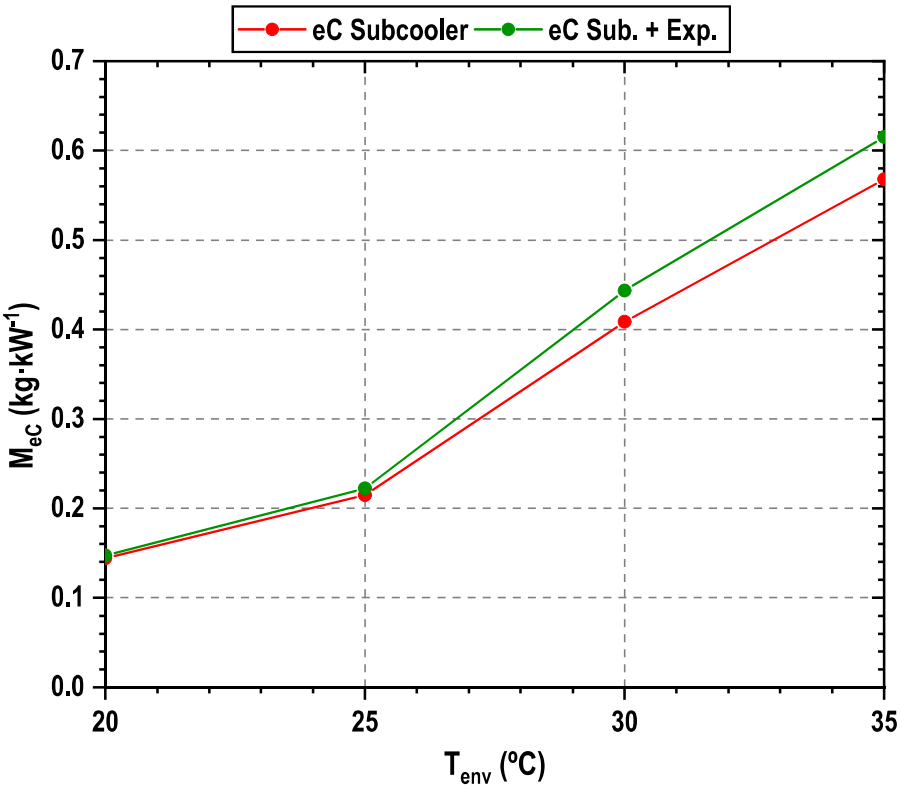

Fig. 9. Mass of eC material per kW of cooling capacity in the main cycle.

Table 3
COP and optimum conditions of different CO_2 systems at 25 °C of heat rejection temperature at $T_o = -15$ °C.

Method	T_{env} (°C)	T_o (°C)	COP	p_{gc} (bar)	SUB (K)	Type	Reference
Parallel compression	24.8	−14.9	1.84	74.4	–	E, O	[40]
Dedicated mechanical subcooling	25.3	−15.5	1.95	74.9	14.3	E, O	[12]
Integrated mechanical subcooling	25.2	−15.6	1.87	74.5	21.3	E, O	[13]
Magnetic refrigeration subcooling	25.0	−15.0	2.10	74.0	9.01	S, O	[11]
Elastocaloric subcooling	25.0	−15.0	2.002	75	4.53	S, O	This work
Elastocaloric subcooling with expander	25.0	−15.0	2.128	75	4.53	S, O	This work

E = Experimental, S = Semiempirical, O = Optimized cycle.

Table 4
COP and optimum conditions of different CO_2 systems at 35 °C of heat rejection temperature at $T_o = -15$ °C.

Method	T_{env} (°C)	T_o (°C)	COP	p_{gc} (bar)	SUB (K)	Type	Reference
Parallel compression	36.3	−15.0	1.25	88.3	–	E, O	[40]
Dedicated mechanical subcooling	35.0	−14.1	1.51	90.0	15.3	E, O	[12]
Integrated mechanical subcooling	35.0	−14.5	1.40	88.4	20.6	E, O	[13]
Magnetic refrigeration subcooling	35.0	−15.0	1.28	88.8	3.6	S, O	[11]
Elastocaloric subcooling	35.0	−15.0	1.40	88.9	6.54	S, O	This work
Elastocaloric subcooling with expander	35.0	−15.0	1.51	88.3	6.54	S, O	This work

E = Experimental, S = Semiempirical, O = Optimized cycle.

elastocaloric device can be used as an external method to subcool the CO_2, getting improvements in the energy performance of the refrigeration system.

The hybrid system has been evaluated at different ambient temperatures from 20 °C to 35 °C for an evaporating level of −15 °C. The system composed of a transcritical single stage CO_2 cycle and the elastocaloric device has been compared to the cycle without subcooling. A third cycle has also been studied: the cycle with eC subcooling and with expander, used to partially recover the energy from the expansion process and used to activate the subcooling device. As other subcooling devices, this system needs to be optimized in terms of subcooling degree and gas-cooler pressure to obtain the maximum COP.

The main obtained results are the COP increments: the eC subcooler provides increments of 2.7 % at 20 °C, 4.5 % at 25 °C, 9.6 % at 30 °C and 13.1 % at 35 °C, while the eC Subcooler + Expander reaches increments of 7.5, 11.1, 18.1 and 22.2 % respectively. The eC Subcooler also allows to reduce the optimum gas-cooler pressure up to 5 bar at the highest environment temperature.

Compared to other subcooling systems used in CO_2 technologies, this new proposal offers competitive values of COP, demonstrating its importance and further potential.

This study shows the need for further improvement of elastocaloric refrigeration devices and proposes a very interesting possible application for them. In addition, in general, transcritical CO_2 VCS introduces high energy irreversibilities in the expansion system, so recovering the energy from the expansion process to activate the subcooling system should also be considered.

Declaration of competing interest

The authors declare that they have no known competing financial interests or personal relationships that could have appeared to influence the work reported in this paper.

Data availability

Data will be made available on request.

Acknowledgements

This article is part of the projects TED2021-130162B-I00, funded by MCIN/AEI/10.13039/501100011033, by the European Union - NextGenerationEU "NextGenerationEU"/PRTR, and FutureECOool funded by University of Ljubljana. Authors want to acknowledge the economic support to this study by the European Union – "NextGenerationEU" (L. Nebot, Margarita Salas postdoctoral contract MGS/2022/15), by the Ministerio de Ciencia e Innovación of Spain (project PID2021-126926OB-C21) and University of Ljubljana (820-1/2020-34). Jaka Tušek would like to acknowledge the support of Slovenian Research Agency (Core funding no. P2-0422).

Appendix A. Supplementary material

Supplementary data to this article can be found online at https://doi.org/10.1016/j.applthermaleng.2024.123843.

References

[1] D.P. Dupont, J.L. Lebrun, P.F. Ziegler, The Role of Refrigeration in the Global Economy, 2019, 38th Note on Refrigeration Technologies, 2019, pp. 12.
[2] J. Steven Brown, P.A. Domanski, Review of alternative cooling technologies, Appl. Therm. Eng. 64 (2014) 252–262.
[3] European Commission, Regulation (EU) No 517/2014 of the European Parliament and of the Council of 16 April 2014 on fluorinated greenhouse gases and repealing Regulation (EC) No 842/2006, 2014.
[4] U. Nations, Amendment to the Montreal Protocol on Substances that Deplete the Ozone Layer, in, Kigali, 2016.
[5] A. Hafner, S. Försterling, K. Banasiak, Multi-ejector concept for R-744 supermarket refrigeration, Int. J. Refrig 43 (2014) 1–13.
[6] L. Nebot-Andrés, D. Calleja-Anta, D. Sánchez, R. Cabello, R. Llopis, Experimental assessment of dedicated and integrated mechanical subcooling systems vs parallel compression in transcritical CO2 refrigeration plants, Energ. Conver. Manage. (2021).
[7] S. Sawalha, M. Karampour, J. Rogstam, Field measurements of supermarket refrigeration systems. Part I: Analysis of CO2 trans-critical refrigeration systems, Appl. Therm. Eng. 87 (2015) 633–647.
[8] R.B. Barta, E.A. Groll, D. Ziviani, Review of stationary and transport CO2 refrigeration and air conditioning technologies, Appl. Therm. Eng. 185 (2021).
[9] R. Llopis, R. Cabello, D. Sánchez, E. Torrella, Energy improvements of CO2 transcritical refrigeration cycles using dedicated mechanical subcooling, Int. J. Refrig. 55 (2015) 129–141.
[10] L. Nebot-Andrés, D. Calleja-Anta, D. Sánchez, R. Cabello, R. Llopis, Experimental assessment of dedicated and integrated mechanical subcooling systems vs parallel compression in transcritical CO2 refrigeration plants, Energ. Conver. Manage. 252 (2022) 115051.
[11] L. Nebot-Andrés, M.G. Del Duca, C. Aprea, A. Žerovnik, J. Tušek, R. Llopis, A. Maiorino, Improving efficiency of transcritical CO2 cycles through a magnetic refrigeration subcooling system, Energ. Conver. Manage. 265 (2022) 115766.
[12] L. Nebot-Andrés, D. Sánchez, D. Calleja-Anta, R. Cabello, R. Llopis, Experimental determination of the optimum working conditions of a commercial transcritical CO2 refrigeration plant with a R-152a dedicated mechanical subcooling, Int. J. Refrig. 121 (2021) 258–268.
[13] L. Nebot-Andrés, J. Catalán-Gil, D. Sánchez, D. Calleja-Anta, R. Cabello, R. Llopis, Experimental determination of the optimum working conditions of a transcritical CO2 refrigeration plant with integrated mechanical subcooling, Int. J. Refrig. 113 (2020) 266–275.

[14] L. Nebot-Andrés, D. Sánchez, R. Cabello, D. Calleja-Anta, C. Fossi, R. Llopis, Current limits of CO2 compressors working in integrated mechanical subcooling cycles, in: 12th International Conference on Compressors and their Systems, London, 2021.
[15] G.F. Peixer, M.C.R. Silva, A. Lorenzoni, G. Hoffmann, D. dos Santos, G.M. do Rosário, E. Pagnan, H.F. Teza, P.M. Silva, S.L. Dutra, M.C. Ribeiro, M.A.A. Rosa, A. Döring, B.P. Vieira, A.T.D. Nakashima, P.A.P. Wendhausen, C.S. Teixeira, J. A. Lozano, J.R. Barbosa, A magnetocaloric air-conditioning system prototype, Int. J. Refrig 151 (2023) 1–13.
[16] IIR, CALORIC COOLING TECHNOLOGIES in: 50th Informatory Note on Refrigeration Technologies, Paris – France, 2022.
[17] I. Takeuchi, K. Sandeman, Solid-state cooling with caloric materials, Phys. Today 68 (2015) 48–54.
[18] S. Fähler, Caloric effects in Ferroic materials: new concepts for cooling, Energ. Technol. 6 (2018) 1394–1396.
[19] Y. Wang, Z. Zhang, T. Usui, M. Benedict, S. Hirose, J. Lee, J. Kalb, D. Schwartz, A high-performance solid-state electrocaloric cooling system, Science 370 (2020) 129–133.
[20] S. Qian, D. Catalini, J. Muehlbauer, B. Liu, H. Mevada, H. Hou, Y. Hwang, R. Radermacher, I. Takeuchi, High-performance multimode elastocaloric cooling system, Science 380 (2023) 722–727.
[21] P. Lloveras, A. Aznar, M. Barrio, P. Negrier, C. Popescu, A. Planes, L. Mañosa, E. Stern-Taulats, A. Avramenko, N.D. Mathur, X. Moya, J.L. Tamarit, Colossal barocaloric effects near room temperature in plastic crystals of neopentylglycol, Nat. Commun. 10 (2019) 1803.
[22] A. Kitanovski, U. Plaznik, U. Tomc, A. Poredoš, Present and future caloric refrigeration and heat-pump technologies, Int. J. Refrig. 57 (2015) 288–298.
[23] M. Masche, J. Liang, K. Engelbrecht, C.R.H. Bahl, Performance assessment of a rotary active magnetic regenerator prototype using gadolinium, Appl. Therm. Eng. 204 (2022) 117947.
[24] J. Chen, K. Zhang, Q. Kan, H. Yin, Q. Sun, Ultra-high fatigue life of NiTi cylinders for compression-based elastocaloric cooling, Appl. Phys. Lett. 115 (2019).
[25] D. Liang, Q. Wang, K. Chu, J. Chen, P. Hua, F. Ren, Q. Sun, Ultrahigh cycle fatigue of nanocrystalline NiTi tubes for elastocaloric cooling, Appl. Mater. Today 26 (2022) 101377.
[26] J. Tušek, K. Engelbrecht, D. Eriksen, S. Dall'Olio, J. Tušek, N. Pryds, A regenerative elastocaloric heat pump, Nat. Energy 1 (2016) 16134.
[27] Ž. Ahčin, S. Dall'Olio, A. Žerovnik, U.Ž. Baškovič, L. Porenta, P. Kabirifar, J. Cerar, S. Zupan, M. Brojan, J. Klemenc, J. Tušek, High-performance cooling and heat pumping based on fatigue-resistant elastocaloric effect in compression, Joule 6 (2022) 2338–2357.
[28] G. Zhou, Y. Zhu, S. Yao, Q. Sun, Giant temperature span and cooling power in elastocaloric regenerator, Joule (2023).
[29] P. Kabirifar, A. Žerovnik, Ž. Ahčin, L. Porenta, M. Brojan, J. Tušek, Elastocaloric Cooling: State-of-the-Art and Future Challenges in Designing Regenerative Elastocaloric Devices 2019 (65) (2019) 16.
[30] Z. Yang, D. Cong, Y. Yuan, R. Li, H. Zheng, X. Sun, Z. Nie, Y. Ren, Y. Wang, Large room-temperature elastocaloric effect in a bulk polycrystalline Ni-Ti-Cu-Co alloy with low isothermal stress hysteresis, Appl. Mater. Today 21 (2020) 100844.
[31] B. Yuan, X. Zhu, X. Zhang, M. Qian, Elastocaloric effect with small hysteresis in bamboo-grained Cu–Al–Mn microwires, J. Mater. Sci. 54 (2019) 9613–9621.
[32] A. Žerovnik, J. Tusek, Hybrid thermal apparatus. WO2018091995A1, 2018-05-24., vol. EP3542108B1, 2016.
[33] A.A. Murthy, A. Subiantoro, S. Norris, M. Fukuta, A review on expanders and their performance in vapour compression refrigeration systems, Int. J. Refrig. 106 (2019) 427–446.
[34] A. Kitanovski, J. Tusek, U. Tomc, U. Plaznik, M. Ozbolt, Magnetocaloric Energy Conversion: From Theory to Applications, Springer, 2015.
[35] E.W. Lemmon, I.H. Bell, M.L. Huber, M. McLinden, REFPROP, NIST Standard Reference Database 23, v.10.0 National Institute of Standards, Gaithersburg, MD, U.S.A., 2018.
[36] P. Gullo, A. Hafner, K. Banasiak, Transcritical R744 refrigeration systems for supermarket applications: current status and future perspectives, Int. J. Refrig 93 (2018) 269–310.
[37] N. Purohit, V. Sharma, S. Sawalha, B. Fricke, R. Llopis, M.S. Dasgupta, Integrated supermarket refrigeration for very high ambient temperature, Energy 165 (2018) 572–590.
[38] P. Aranguren, D. Sánchez, A. Casi, R. Cabello, D. Astrain, Experimental assessment of a thermoelectric subcooler included in a transcritical CO2 refrigeration plant, Appl. Therm. Eng. 190 (2021) 116826.
[39] D. Sánchez, P. Aranguren, A. Casi, R. Llopis, R. Cabello, D. Astrain, Experimental enhancement of a CO2 transcritical refrigerating plant including thermoelectric subcooling, Int. J. Refrig 120 (2020) 178–187.
[40] L. Nebot-Andrés, D. Sánchez, D. Calleja-Anta, R. Cabello, R. Llopis, Experimental determination of the optimum intermediate and gas-cooler pressures of a commercial transcritical CO2 refrigeration plant with parallel compression, Appl. Therm. Eng. (2021).